Structural phase-transition study by Gd^{3+} EPR of $Sm(BrO_3)_3.9H_2O$ and $Nd(BrO_3)_3.9H_2O$ single crystals

1990 J. Phys.: Condens. Matter 2 5603

(http://iopscience.iop.org/0953-8984/2/25/012)

J. Phys.: Condens. Matter 2 (1990) 5603–5611. Printed in the UK

Structural phase-transition study by Gd^{3+} EPR of $Sm(BrO_3)_3 \cdot 9H_2O$ and $Nd(BrO_3)_3 \cdot 9H_2O$ single crystals

Sushil K Misra†§, Gérard Bacquet‡ and Jean Frandon‡

† Physics Department, Concordia University, 1455 de Maisonneuve Boulevard West, Montreal, Quebec H3G 1M8, Canada

‡ Laboratoire de Physique des Solides, Associé au CNRS (UA74), 118 route de Narbonne, 31062 Toulouse Cédex, France

Received 12 February 1990, in final form 29 March 1990

Abstract. X-band (≃ 9.25 GHz) EPR measurements on single crystals of Gd^{3+}-doped $Sm(BrO_3)_3 \cdot 9H_2O$ (SmBR) and $Nd(BrO_3)_3 \cdot 9H_2O$ (NdBR) have been performed in the temperature range 4–295 K. It is found that the crystals of SmBR and NdBR undergo structural phase transitions of second order at 38.5 K and 29 K, respectively. The spin-Hamiltonian parameters for one of the two magnetically inequivalent Gd^{3+} ions in the unit cell have been estimated, using a least-squares fitting program, at 295, 115, and 30 K for SmBR, and at 295, 140, and 60 K for NdBR. The general features of the EPR spectra for the two crystals are the same over the temperature range investigated; the absolute value of the zero-field splitting parameter, b_2^0, increases as the temperature is decreased.

1. Introduction

To date no electron paramagnetic resonance (EPR) study as been reported either on Gd^{3+}-doped samarium bromate nonahydrate, $Sm(BrO_3)_3 \cdot 9H_2O$ (SmBR hereafter), or on Gd^{3+}-doped neodynium bromate nonahydrate, $Nd(BrO_3)_3 \cdot 9H_2O$ (NdBR hereafter). Further, the crystal structures of the rare earth bromate nonahydrates (RBR) have been erroneously believed to be similar to those of the rare-earth ethylsulphate nonahydrates, $R(C_2H_5SO_4)_3 \cdot 9H_2O$ (R = rare-earth, RES hereafter). (See section 2 for more details.) The EPR of Gd^{3+}-doped RES single crystals has been extensively studied (Misra *et al* 1986), while only three EPR studies have been reported recently on Gd^{3+}-doped RBR; specifically on $Pr(BrO_3)_3 \cdot 9H_2O$ by Bacquet *et al* (1990), and on $La(BrO_3)_3 \cdot 9H_2O$ by Washington (1982) and by Krygin *et al* (1988). Both the observation of Bacquet *et al* (1970) and Washington (1982) indicate that Gd^{3+} EPR spectrum in RBR is different from that in RES. Specifically, when the Zeeman field is parallel to the pseudohexagonal axis the EPR spectra in RBR were not characterised by a mirror symmetry of the seven Gd^{3+} lines across the central line, typical of Gd^{3+} spectra in RES. It appears that the RBR crystals used for these investigations were triply-twinned hexagonal columns. (More details are described by Bacquet *et al* (1990).)

§ On leave of absence at Laboratoire de Physique des Solides, associé au CNRS (UA74), Université Paul Sabatier, Toulouse, France (November 1 1989–January 31 1990).

0953-8984/90/255603 + 09 $03.50

In an attempt to study Gd^{3+}-doped RBR crystals systematically, to facilitate understanding of the origin and crystal-field effects, the present paper reports the first-ever EPR study on Gd^{3+}-doped single crystals of SmBR and NdBR. The spin-Hamiltonian parameters of Gd^{3+}, so determined, can be used for a theoretical analysis to understand the crystal fields experienced by the Gd^{3+} ion in the lattices of SmBR and NdBR. The Gd^{3+} ion, characterised by the ground state $^8S_{7/2}$, readily yields well-resolved EPR spectra over the temperature range of liquid helium to room temperature. It turns out, from the present measurements, that the SmBR and NdBR crystals undergo structural phase transitions (SPT) over this temperature range. Thus, the SPT of these crystals can be studied by EPR, which is very sensitive to the changes in the environment surrounding the paramagnetic ion used as a probe.

The preparation and the structure of the samples, along with the experimental details, are described in section 2. The details of the EPR spectra, in the temperature range investigated, are given in section 3. This is followed by the evaluation of spin-Hamiltonian parameters in section 4. Section 5 deals with the comparison of the present EPR results on Gd^{3+}-doped SmBR and NdBR with those on RES.

2. Crystal structure and experimental details

According to the x-ray diffraction studies (Albertsson and Elding 1977) RBR crystallise in the space group $P6_3/mmc$ with $Z = 2$. The values of the unit-cell parameters are: $a = 1.17885$ nm, $c = 0.67511$ nm for SmBR; $a = 1.18224$ nm, $c = 0.67858$ nm for NdBR. However, it is now generally recognised that RBR crystals are pseudohexagonal, and not hexagonal as indicated by diffraction studies of Albertsson and Elding (1977) and of Sikka (1969). This is evidenced by optical absorption studies of Hellwege and Hellwege (1950) and Hellwege and Kahle (1951), and more recently by Poulet *et al* (1975). The difficulty of Albertsson and Elding (1977) in detecting the twinning inherent in the pseudohexagonal structure and some doubt that all members of RBR family shared this structural feature have tended to perpetuate the idea that all RBR crystals should be quite similar to the corresponding ethylsulphates, RES. Magnetic measurements by Simizu *et al* (1984) disproved this. Accordingly, Taylor and Sussums (1985) studied EPR of Nd^{3+} in PrBR, leading to the detection of inequivalent R^{3+} sites in these crystals, as well as the lowering of site symmetry from D_{3h}. A review of crystal structure of RBR is given by Gerkin and Reppart (1987). It is noted that continuous structural phase transitions have been detected calorimetrically in a number of RBR compounds near 66 K (Poulet *et al* 1975 and Simizu *et al* 1986). To summarise, the previous studies suggest that the RBR crystals are biaxial, but display pseudohexagonal symmetry. Crystals of some of the salts are composed on six triangular sections, twinned in such a manner that the external form of the crystal is a hexagonal column. The pseudohexagonal character of the crystals decrease with temperature down to 65 K, at which temperature a phase transition occurs. Below 65 K, the symmetry at the site of the rare-earth ion is triclinic, and there are several inequivalent rare-earth ions in the unit cell. Above the phase-transition temperature, there is $\bar{2}$ (= m) symmetry at the rare earth-ion site. The mirror plane contains the paendohexagonal axis, and is parallel to the prism face of the triangular section. The crystal field at the rare earth-ion site is predominantly determined by the water molecules surrounding the rare-earth ion, with the bromate ions having only a small influence. The symmetry of the crystal field is therefore determined predominantly by the symmetry of the hydrated ion.

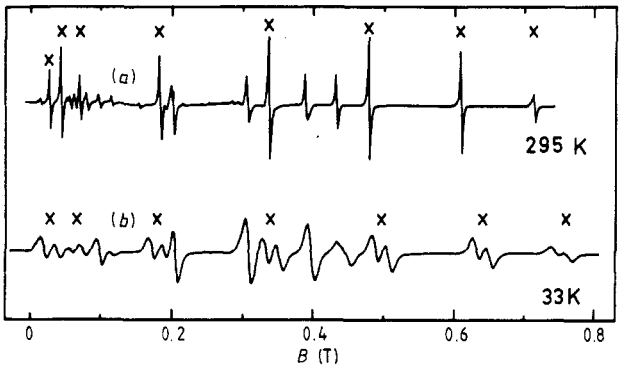

Figure 1. First-derivative X-band ($\simeq 9.25$ GHz) EPR spectra for $\boldsymbol{B} \parallel \hat{Z}$ for Gd^{3+}-doped $Sm(BrO_3)_3 \cdot 9H_2O$ single crystal at (*a*) 295 and (*b*) 33 K. The X's represent the lines belonging to Gd^{3+} ion I. (Note that the lowest-magnetic-field forbidden transition that occurs at 295 K is not observed at 33 K.)

Single crystals of SmBR and NdBR were prepared by slow evaporations of the respective aqueous solutions, to which sufficient amounts of $Gd(BrO_3)_3 \cdot 9H_2O$ powder were added, so that there was one Gd^{3+} ion per 1000 Sm^{3+}, or Nd^{3+}, ions. The crystals were hexagonal prisms, bounded by {100} and {011} faces, being light yellow and light pink for SmBR and NdBR, respectively.

An E-line Century series X-band Varian spectrometer, with a 25 kHz modulation, was employed to carry out the measurements. An ESR 900 Oxford Instruments continuous-flow cryostat (4–300 K) was fitted to the high-Q Varian TE_{102} cavity. The sample could be rotated, with a precision of $\pm 0.5°$, about an axis perpendicular to the static magnetic (Zeeman) field. The calibration of the magnetic-field values was accomplished by proton resonance.

3. EPR spectra

(*i*) *Room temperature.* Figure 1(*a*) exhibits the EPR spectrum, recorded at 295 K, for SmBR for the orientation of the Zeeman field ($\boldsymbol{B}$) along the principal Z axis of one of the two magnetically-inequivalent Gd^{3+} ions (Gd^{3+} ion I) in the unit-cell of SmBR. (The magntic Z, X, Y axes of the impurity ion Gd^{3+} are those directions of $\boldsymbol{B}$ for which the overall splitting of EPR lines exhibit extrema, the overall splittings being successively greater for $\boldsymbol{B} \parallel \hat{Y}, \hat{X}, \hat{Z}$.) For Gd^{3+} ion I, two magnetic axes were found to lie in the {100} plane of the crystal, as identified unequivocally by the perfect symmetry of the EPR lines about them. By comparison with the EPR spectrum of SmBR powder it was found that one of these axes is the Z axis. Further, comparison with the Gd^{3+} EPR spectra in other host crystals exhibiting orthorhombic site symmetry, revealed that the second axis is the Y axis, and not the X axis; for, the overall splitting for $\boldsymbol{B} \parallel \hat{X}$ is much larger than that for $\boldsymbol{B} \parallel \hat{Y}$. In the absence of an arrangement where the crystal could be rotated about two mutually perpendicular axes, it was not possible to determine the orientations of the magnetic axes corresponding to Gd^{3+} ion II in the unit-cell.

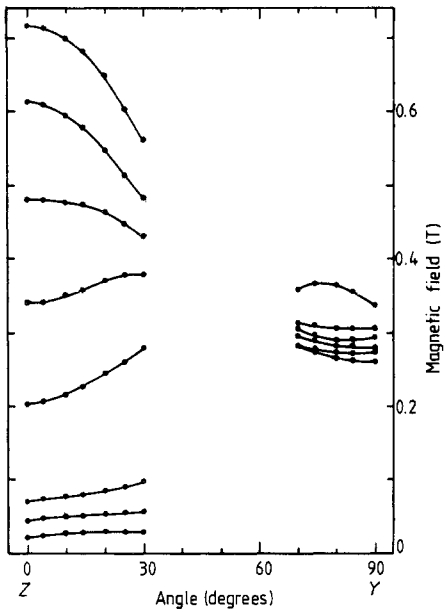

Figure 2. Angular variation of the EPR line positions for Gd^{3+} ion I in the SmBR host crystal for $\boldsymbol{B}$ in the ZY plane (coincident with the {100} plane) at 295 K. Only the line positions over intervals of 30° and 20° from the Z and Y axes, respectively, have been plotted. The superposition by EPR lines of Gd^{3+} ion II does not allow unequivocal identification of the lines belonging to Gd^{3+} ion I at intermediate angles. The continuous lines connect data points corresponding to the same transition. The SMD value of table 1 indicates that the calculated line positions differ, on the average, by about 1% from those measured experimentally.

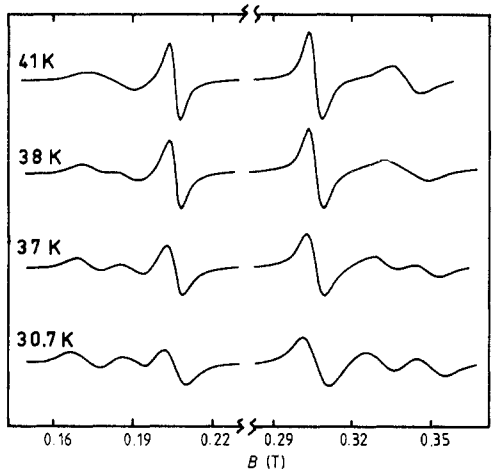

Figure 3. Part of Gd^{3+} EPR spectra for $\boldsymbol{B} \parallel \hat{Z}$ in the SmBR host in the temperature interval 30.7–41 K. Below the phase-transition temperature, T_c, each of the lines belonging to Gd^{3+} ion I splits into two. Thus T_c is deduced to be 37.5 ± 0.5 K for SmBR.

The angular variation of the EPR line positions for $\boldsymbol{B}$ in the ZY plane of Gd^{3+} ion I for SmBR is depicted in figure 2. Similar details of EPR spectra and angular dependence were found to be true for NdBR single crystals at room temperature.

(*ii*) *Lower temperatures.* It was found, upon lowering the temperature down to the respective T_c, the phase-transition temperature, that the general features of the EPR spectra for each of SmBR and NdBR, for various orientations of $\boldsymbol{B}$, remained the same. However, the overall splitting of the EPR lines increased with lowering of temperature, indicating a monotonic increase in the absolute value of the zero-field splitting parameter, b_2^0. This was accompanied by broadening of linewidths, as explained later.

(iii) Below T_c (phase transition). Below the phase-transition temperature $T_c = 38 \pm 0.5$ K for SmBR and $T_c = 29.0 \pm 0.5$ K for NdBR, the EPR spectra changed gradually for the two hosts, such that each EPR line for Gd^{3+} ion I, and not for Gd^{3+} ion II, split into two well-resolved lines, as is clearly seen, e.g., in figure 1(*b*) for SmBR. Part of the Gd^{3+} EPR spectra above and below T_c for SmBR for $\boldsymbol{B} \parallel \boldsymbol{Z}$ is shown in figure 3; a

similar behaviour is observed for NdBR. This indicates that the structural phase transitions experienced by SmBR and NdBR are of second order. The splitting of each Gd^{3+} ion I EPR line with temperature (T) was found to vary in accordance with the critical behaviour $(T_c - T)^{0.5}$ (Waplak *et al* 1986, Müller and Berlinger 1971) for $T < T_c$ in a region of 5 K within T_c, below which the splittings of the lines did not change significantly. As the temperature was lowered further, the overall features of the spectra remained the same down to 4 K. However, numerous EPR lines, due to Sm^{3+} ions appeared below 24 K in the SmBR host, which masked considerably the Gd^{3+} EPR spectra. The same was found to be true for the NdBR host, except that fewer Nd^{3+} EPR lines than those of Sm^{3+} in the SmBR host, appeared below 28 K.

(*iv*) *EPR linewidth.* For SmBR, the peak-to-peak first-derivative linewidth, ΔB_{pp}, was found to be independent of the magnitude and orientation of $\boldsymbol{B}$. However, it increased as the temperature was decreased. ΔB_{pp} of the third highest-field line for this host for $\boldsymbol{B} \parallel \hat{Z}$ of Gd^{3+} ion I (located at about 0.5 T in figure 1(*a*)) was observed to be 2.1 ± 0.2 mT, 2.6 ± 0.2 mT, 7.6 ± 0.5 mT, 8.9 ± 1.0 mT, 11.5 ± 1.0 mT and 14.6 ± 1.0 mT at 295, 194, 39, 37, 28 and 25 K, respectively. (The values below T_c are those of one of the split lines.) Below 25 K, the presence of EPR lines due to the host Sm^{3+} ions masked the Gd^{3+} lines considerably, making it impossible to measure ΔB_{pp} for Gd^{3+}.

In the case of NdBR, it was found that ΔB_{pp} depended both on the orientation, and magnitude, of $\boldsymbol{B}$, i.e., the values of ΔB_{pp} were different for transitions occurring at different values of $\boldsymbol{B}$, as well as for transitions occurring at different orientations of $\boldsymbol{B}$. This is at variance with observations in SmBR. Further, ΔB_{pp} increased for any EPR line as the temperature was lowered. To give an idea of ΔB_{pp} for Gd^{3+} in NdBR, for the same third highest-field line for $\boldsymbol{B} \parallel \hat{Z}$ as that in SmBR, ΔB_{pp} was measured to be 2.2 ± 0.2 mT, 6.3 ± 0.5 mT, $17.1 \pm 1{,}0$ mT, 19.2 ± 1.0 mT, 19.7 ± 1.0 mT and 21.0 ± 1.0 mT at 295, 140, 43, 34, 22, and 4 K, respectively. As the intense Nd^{3+} lines, which appeared below 28 K, did not overlap the particular Gd^{3+} line considered, it was, indeed, possible to measure ΔB_{pp} for Gd^{3+} ion I down to 4 K.

The observed temperature variation of ΔB_{pp} can be understood as follows. ΔB_{pp} is a direct measure of the host ion (Nd^{3+} or Sm^{3+} in the present case) spin-lattice relaxation time τ_1'. It has been shown, taking into account the dipole–dipole and exchange interactions between the impurity ion (Gd^{3+} in the present case) and the host ions (Misra and Orhun 1989) that

$$\tau' = 3g\mu_B \Delta B_{pp} f / 110.45 \overline{\langle \Delta\nu^2 \rangle} h \tag{3.1}$$

where $f = 1.75$ for the Lorentzian lineshape and $f = 1.18$ for the Gaussian lineshape, g is the Gd^{3+} ion g factor, μ_B is the Bohr magneton and h is Planck's constant. In (3.1) $\langle \Delta\nu^2 \rangle$ is the second moment, expressed as (Misra and Orhun 1989):

$$\overline{\langle \Delta\nu^2 \rangle} = \tfrac{1}{3} S'(S'+1) h^{-2} (NJ^2 + (gg')^2 \mu_B^4 \mu_0^2 \sum_{k'}^{N} (1 - 3\cos^2 \theta_{jk'})^2 r_{jk'}^{-6}$$

$$+ 2Jgg' \mu_B^2 \mu_0 \sum_{k'}^{N} (1 - 3\cos^2 \theta_{jk'}) r_{jk'}^{-3}). \tag{3.2}$$

In (3.2) J is the effective pair exchange-interaction constant between the pair of host-impurity ions; N is the number of nearest and next-nearest neighbour ions; g', S and S' are, respectively, the g factor for the host ion, the electronic spin of the impurity ion,

and the electronic spin of the host ion; $\boldsymbol{r}_{jk'}$ is the vector that joins the impurity ion to the host in k'; $\theta_{jk'}$ is the angle between $\boldsymbol{r}_{jk'}$ and $\boldsymbol{B}$; and μ_0 ($= 1.26 \times 10^{-6}$ H m^{-1}) is the magnetic permeability constant. Equation (3.2) takes into account, appropriately, the dipole–dipole and exchange interactions between the impurity Gd^{3+} ion and the host ion, Sm^{3+} or Nd^{3+}.

From (3.1), it is seen that the dependence of τ_1' on temperature (T) is predominantly the same as that of ΔB_{pp} on T, since the dependence of $\overline{\langle \Delta\nu^2 \rangle}$, which in turn depends on $r_{jk'}$ and J, on temperature is usually not too drastic. Thus, from the observed ΔB_{pp} versus T behaviour one can estimate the value of the power n in the relation $\tau' \simeq T^{-n}$. Accordingly, it is found that for Sm^{3+} ions in SmBR $n = 0.5 \pm 0.1$ for $194 \leqslant T \leqslant 295$ K, and $n = 1.1 \pm 0.1$ for $T \leqslant 39$ K, while for Nd^{3+} ions in NdBr $n = 1.0 \pm 0.1$ for $40\text{ K} \leqslant T \leqslant 295$ K and $n = 0.04 \pm 0.01$ for $T \leqslant 34$ K. Detailed calculations show that $n \geqslant 2$ for the well-known processes, such as Raman, Orbach, the three-phonon, the local mode, or the collision processes (Shrivastava 1983). However, in the present case $n \leqslant 1.1$ at all temperatures of investigation. Thus, these well-known processes do not explain the observed ΔB_{pp} versus T behaviours. On the other hand, a satisfactory explanation of the present results can be provided by a detailed computation using the Monte Carlo technique, taking into account the dipolar interactions between the impurity Gd^{3+} ion and the host, Sm^{3+} or Nd^{3+}, ions. Since, the present results are similar to those for Gd^{3+}-doped $Yb_xY_{1-x}Cl_3 \cdot 6H_2O$ crystals, for which such a technique has been successfully applied (Misra *et al* 1988).

3.1. Comparison with PrBR

At 295 K the general features of the EPR spectra for PrBR (Bacquet *et al* 1990) are the same as those for SmBR and NdBR. The Z, Y axes for Gd^{3+} ion I are oriented in the {100} plane of the three RBR hosts studied. Unlike SmBR and NdBR, PrBR crystal does not undergo any structural phase transition in the 4–295 K temperature range. This may perhaps be due to the differences in the strengths of the interactions of the Pr^{3+}, Sm^{3+} and Nd^{3+} ions with the surrounding ligands, i.e., the bromate ions and the water molecules. The overall splitting of the EPR lines are found to be about the same in the three hosts; also, the magnitude of the paramater b_2^0 increased for all these hosts as the temperature was lowered.

4. Spin Hamiltonian and evaluation of parameters

The line positions for Gd^{3+} ion I, as observed for $\boldsymbol{B}$ in the ZY plane for both SmBR and NdBR, are characteristic of orthorhombic site symmetry. They were, thus, fitted to the following spin Hamiltonian

$$\mathcal{H} = \mu_B(g_{zz}B_zS_z + g_{yy}B_yS_y) + \frac{1}{3}\sum_{m=0,2} b_2^{m'}O_2^m + \frac{1}{60}\sum_{m=0,2,4} b_4^{m'}O_4^m + \frac{1}{1260}\sum_{m=0,2,4,6} b_6^{m'}O_6^m \tag{4.1}$$

In (4.1) μ_B is the Bohr magneton, $S(= 7/2)$ is the electronic spin of Gd^{3+}, O_l^m are the spin operators (Abragam and Bleaney 1970) and g_{zz}, g_{yy}, $b_l^{m'}$ are the spin Hamiltonian parameters (SHP).

Table 1. The spin-Hamiltonian parameters (SHP) for Gd^{3+} ion I in the SmBR host at various temperatures. The units of b_l^m are GHz, while the g-values are dimensionless. Here SMD $(GHz^2) \equiv \Sigma_i(|\Delta E_i| - h\nu_i)^2$, where the summation is over the n line positions fitted simultaneously to evaluate the SHP; ΔE_i and ν_i are, respectively, the separation of the energy levels participating in resonance for the ith line position and the corresponding klystron frequency; and h is Planck's constant. The parameter errors are estimated by the use of a statistical method (Misra and Subramanian 1982). The absolute sign of b_2^0 has been assumed to be negative in accordance with that for PrBR; the relative signs of all b_l^m are correct.

Parameter	295 K	115 K	30 K
g_{zz}	1.9980 ± 0.0006	1.9949 ± 0.0007	1.9863 ± 0.0009
g_{yy}	1.998 ± 0.001	1.997 ± 0.001	1.989 ± 0.002
b_2^0	−1.950 ± 0.001	−2.033 ± 0.001	−2.024 ± 0.001
b_2^2	1.279 ± 0.002	0.849 ± 0.002	0.830 ± 0.002
b_4^0	0.0485 ± 0.0003	0.0370 ± 0.0003	0.0438 ± 0.0004
b_4^2	−0.064 ± 0.002	0.021 ± 0.002	−0.005 ± 0.002
b_4^4	−0.360 ± 0.003	0.002 ± 0.003	−0.083 ± 0.004
b_6^0	−0.0108 ± 0.0002	0.0024 ± 0.0002	−0.0099 ± 0.0002
b_6^2	0.000 ± 0.002	0.089 ± 0.002	0.093 ± 0.002
b_6^4	−0.148 ± 0.002	0.117 ± 0.003	−0.136 ± 0.004
b_6^6	−0.059 ± 0.008	−0.124 ± 0.004	−0.211 ± 0.005
n	93	88	63
SMD	1.29	0.72	0.76

All EPR line positions, belonging to Gd^{3+} ion I, for $\boldsymbol{B}$ in the ZY plane, were simultaneously fitted, using a least-squares fitting (LSF) procedure (Misra 1976), diagonalising the SH matrix on a digital computer, to evaluate the SHP for SmBR and NdBR. For temperatures below T_c, the averages of the line positions of the doubly-split lines corresponding to Gd^{3+} ion I were used. The errors were estimated by the use of a statistical method (Misra and Subramanian 1982). In (1), the SHP, $b_l^{m'}$ have been defined in the ZY principal axes system. Their relations to b_l^m, defined in the ZX principal-axes system, are: $b_l^{m'} = b_l^m$ for all l, m, except for l, 2 and l, 6 for which $b_l^{m'} = -b_l^m$. Therefore, the values of the SHP, as listed in tables 1 and 2, for SmBR and NdBR, respectively, are those for b_l^m, as derived from $b_l^{m'}$, using these relations. Only the relative signs of b_l^m, as given in these tables, are correct: the absolute signs could not be determined because of the overlap of Gd^{3+} lines by the host ion, Sm^{3+} or Nd^{3+}, lines at liquid-helium temperature, since it is the intensity of the higher-field lines relative to the lower-field EPR lines at liquid-helium temperature that determines the absolute signs of b_2^0 (Abragam and Bleaney 1970). The signs of b_2^0 in tables 1 and 2 have been assumed to be negative, in accordance with that in PrBR (Bacquet *et al* 1990). The relative signs of the parameters, as yielded by LSF method, are, however, correct.

5. Discussion and concluding remarks

The structural phase transitions as indicated by the splitting of the EPR lines corresponding to Gd^{3+} ion I, and not to ion II, below T_c in the SmBR and NdBR host crystals indicate that, below T_c, the unit cell modifies itself in such a way that there are two magnetically inequivalent ions corresponding to Gd^{3+} ion I, whose environments

Table 2. The SHP for Gd^{3+}-doped NdBR single crystal. For notations and other details, including the signs of b_l^m, refer to the caption of table 1.

Parameter	295 K	140 K	60 K
g_{zz}	1.9817 ± 0.0005	2.0029 ± 0.0008	2.0117 ± 0.0009
g_{yy}	2.0108 ± 0.0008	2.008 ± 0.001	2.054 ± 0.001
b_2^0	−1.8603 ± 0.0007	−2.075 ± 0.001	−2.131 ± 0.001
b_2^2	1.011 ± 0.001	1.016 ± 0.002	1.087 ± 0.003
b_4^0	0.0259 ± 0.0002	0.0404 ± 0.0004	0.0402 ± 0.0004
b_4^2	0.079 ± 0.002	−0.008 ± 0.002	−0.022 ± 0.002
b_4^4	0.100 ± 0.002	0.004 ± 0.003	−0.095 ± 0.005
b_6^0	0.0032 ± 0.001	−0.0019 ± 0.0002	−0.0110 ± 0.0003
b_6^2	−0.013 ± 0.002	−0.007 ± 0.002	0.021 ± 0.002
b_6^4	0.027 ± 0.002	−0.096 ± 0.002	0.193 ± 0.003
b_6^6	0.104 ± 0.003	0.392 ± 0.005	0.083 ± 0.006
n	141	90	58
SMD	1.21	0.79	0.81

are only slightly different from each other. That this does not happen for ion II is only indicated by the orientation of $\boldsymbol{B}$ in the ZY plane. It may be possible that the same is true of ion II, except that the resulting two ions are magnetically equivalent with respect to the ZY plane of ion I.

As for comparison of the EPR results on Gd^{3+}-doped SmBR and NdBR with those on Gd^{3+}-doped RES, the following similarities/differences may be noted:

(i) The EPR spectra for RES in the range 4–295 K are due to the presence of two magnetically equivalent Gd^{3+} ions in the unit cell, while in the SmBR and NdBR hosts they are due to the presence of two magnetically-inequivalent Gd^{3+} ions at $T > T_c$, and at least three magnetically-inequivalent Gd^{3+} ions at $T < T_c$, in the unit cell.

(ii) The EPR spectra in the RES hosts exhibit axial symmetry about the c axis. This is not at all true for the SmBR and NdBR hosts. This difference can be easily understood by the differences in the R^{3+} site symmetry in the two hosts as described in sections 1 and 2.

(iii) While the SmBR and NdBR crystals undergo phase transitions in the 4–295 K temperature range, no phase transition is experienced by the RES crystals in this range.

(iv) The absolute value of the zero-field splitting parameter, b_2^0, increases in all, SmBR, NdBR and RES host crystals when the temperature is lowered.

(v) The Gd^{3+} EPR linewidth in the RES hosts, SmES and NdES, exhibit the same general trends with respect to temperature, as those in the corresponding hosts SmBR and NdBR (Gerkin and Thorsell 1972). Further, the linewidths are not too dependent on the magnitude of $\boldsymbol{B}$ (different transitions) for SmES, while they do depend rather significantly on the magnitude of $\boldsymbol{B}$ for NdES. ΔB_{pp} increases with decreasing temperature for the NdES host and remains about the same for the SmES host. The only difference betrween the ΔB_{pp} of the two particular RES and RBR hosts is that the values of ΔB_{pp} are significantly smaller in the RES hosts, as compared to those in the corresponding RBR hosts, given in section 3(iv). In particular, for the third highest-field line for $\boldsymbol{B} \parallel \hat{Z}$, $\Delta B_{pp} = 0.64 \pm 0.06$ mT and 5.8 ± 0.6 mT for SmES at 295 and 77 K respectively, while $\Delta B_{pp} = 0.83 \pm 0.08$ mT and 3.2 ± 0.3 mT at 295 and 77 K respectively for NdES (Gerkin and Thorsell 1972). The difference of ΔB_{pp} behaviour between

these particular RBR and the corresponding RES hosts can be easily explained if it is realised that the separations of the rare-earth ions in RES is significantly larger than those in the RBR hosts. This considerably diminishes the strength of the dipolar interactions, which is inversely proportional to the cube of the distance, between the rare-earth ions in the RES hosts as compared to those in the RBR hosts. (The unit cell parameters for SmES are a = 1.39884 nm, c = 0.70909 nm, while for NdES they are a = 1.40275 nm, c = 0.71130 nm; Albertsson and Elding 1977.)

Acknowledgments

One of us (SKM) is grateful to the Natural Sciences and Engineering Research Council of Canada (NSERC) for awarding an international collaborative grant to spend part of his sabbatical year at the Laboratoire de Physique des Solides, Univesité Paul Sabatier, Toulouse, France, where this research was performed. He thanks this laboratory, and especially Dr Bacquet, for the hospitality extended during his sojourn in Toulouse, France. We are grateful to Dr L E Misiak for growing the crystals used in the present study.

References

Abragam A and Bleaney B 1970 *Electron Paramagnetic Resonance of Transition Ions* (Oxford: Clarendon) p 863
Albertsson J and Elding I 1977 *Acta Crystallogr.* B **33** 1460
Bacquet G, Misra S K, Misiak L E and Fabre F 1990 *Solid State Commun.*
Gerkin R E and Reppart W J 1987 *Acta Crystallogr.* C **43** 623
Gerkin R E and Thorsell D L 1972 *J. Chem. Phys.* **57** 2665
Hellwege A M and Hellwege K H 1950 *Z. Phys.* **127** 334
Hellwege K H and Kahle H G 1951 *Z. Phys.* **129** 85
Krygin I M, Prokhorov A D and Chernysh L F 1988 *Sov. Phys. – Crystallogr.* **33** 461
Misra S K 1976 *J. Magn. Reson.* **23** 403
Misra S K and Orhun U 1989 *Phys. Rev.* B **39** 2856
Misra S K, Orhun U and Daniels J M 1988 *Phys. Rev.* B **38** 8683
Misra S K and Subramanian S 1982 *J. Phys. C: Solid State Phys.* **15** 7199
Misra S K and Upreti G C 1986 *Magn. Reson. Rev.* **10** 333
Müller K A and Berlinger W 1971 *Phys. Rev. Lett.* **26** 13
Poulet H, Mathieu J P, Vergnat D, Hadni A and Gerbaux X 1975 *Phys. Status Solidi* a **32** 509
Shrivastava K N 1983 *Phys. Status Solidi* b **117** 437
Sikka S K 1969 *Acta Crystallogr.* A **25** 621
Simizu S, Bellesis G H and Friedberg S A 1984 *J. Appl. Phys.* **55** 2333
—— 1986 *J. Magn. Magn. Mater.* **54–57** 1331
Taylor D R and Sussums A A F 1985 *J. Appl. Phys.* **57** 3736
Waplak S, Schmidt V H and Drumheller J E 1986 *Phys. Rev.* B **34** 6532
Washington N M 1982 *PhD Thesis* Ohio State University